Improvement of Unmanned Aerial Vehicle Object Detection Through Scale Optimization and YOLOv7-Tiny Anchor Adjustment

Febrianto Eko Saputra and Ingrid Nurtanio
Department of Informatics, Hasanuddin University, Indonesia

Keywords: Object Detection, YOLOv7-Tiny, UAV, Small Objects, Anchor Box.

Abstract: Object detection in Unmanned Aerial Vehicle (UAV) images is challenging due to variations in scale, shooting angle, and object density, particularly for small objects. YOLOv7-Tiny, a lightweight real-time model, offers high efficiency but limited accuracy in this scenario. This study proposes architectural modifications and anchor optimization to enhance detection performance. The architecture is improved by adding a high-resolution detection path to the neck and an additional detection layer to the head, thereby strengthening small object feature representation. Furthermore, anchor box optimization using the K-means algorithm with Manhattan Distance produces anchors that are more representative of the UAV dataset's object size distribution. Experimental results show that the optimized YOLOv7-Tiny achieves stable precision (95) and recall (96), with the F1-Score increasing from 95 to 96 compared to the baseline. The model also improves mAP at low to medium IoU thresholds, raising the average mAP@50–95 from 71.68 to 72.73. However, performance decreases at high IoU thresholds, and inference time slightly increases due to added complexity. Overall, the proposed approach improves UAV small object detection with a trade-off in processing efficiency.

1 INTRODUCTION

Object detection is one of the core tasks in the field of computer vision, with various strategic applications such as military operations, autonomous vehicles, security monitoring systems, and remote observation. In recent years, the use of unmanned aerial vehicles (UAVs) (Mohsan et al., 2022) as platforms for aerial imaging has grown rapidly across various sectors, due to their ability to capture images over large areas, making them a highly promising source of data for supporting various object detection tasks (Ali & Zhang, 2024). However, the unique characteristics of aerial images captured by UAVs, such as variations in distance and angle of capture, pose a number of challenges in the object detection process. One of the main problems is the wide range of target sizes. Large objects, such as cars at close range, are relatively easy to detect, while smaller and denser objects, such as bicycles or pedestrians, are often difficult to identify accurately. Additionally, the limitations of UAVs in terms of payload capacity and portability make it challenging to integrate high-performance computing hardware, thereby restricting real-time processing capabilities on the UAV platform itself (Xiao & Di, 2024).

To address these challenges, various deep learning-based object detection algorithms have been developed and implemented on UAV images. In general, modern detection algorithms can be divided into two main categories based on their architecture, namely two-stage and one-stage algorithms (Bi et al., 2023). Two-stage algorithms, such as Faster R-CNN (Xu et al., 2022), perform the detection process in two steps: first, generating candidate regions using selective search and feature extraction; second, classifying and refining the object locations. Although this method achieves high accuracy, its complex structure makes it less efficient for real-time applications on UAVs. In contrast, single-stage algorithms like the You Only Look Once (YOLO) (Badgujar et al., 2024) series combine feature extraction and object location and category prediction directly in a single step, making them significantly more efficient (S. Liu et al., 2025). However, YOLO still shows limitations in detecting small objects in UAV images. This is due to weak representation of small object features and loss of spatial information at low resolution levels. Therefore, optimization of network architecture and model parameters is needed to improve the accuracy of small object detection in complex UAV

Eko Saputra, F. and Nurtanio, I.
Improvement of Unmanned Aerial Vehicle Object Detection Through Scale Optimization and YOLOv7-Tiny Anchor Adjustment.
DOI: 10.5220/0014268500004928

In *Proceedings of the 1st International Conference on Research and Innovations in Information and Engineering Technology (RITECH 2025)*, pages 37-44
ISBN: 978-989-758-784-9

imaging conditions (Telçeken et al., 2024).

Among the various single-stage detection algorithms available today, YOLOv7 (C.-Y. Wang et al., 2023) stands out as one of the most reliable and efficient methods in terms of detection accuracy and speed. YOLOv7-tiny (Q. Wang et al., 2024), as a lightweight variant of YOLOv7, is specifically designed for applications on edge devices with limited computational resources. Compared to other YOLOv7 variants, YOLOv7-tiny offers fewer parameters and faster inference times, making it suitable for deployment on UAV platforms that demand computational efficiency and real-time detection. Although its detection accuracy is slightly lower than the full version of YOLOv7, this trade-off is acceptable within the constraints of UAV hardware limitations (Zhang et al., 2024). In the YOLOv7-Tiny architecture, the head component plays an important role in generating predictions based on features extracted by the backbone. By utilizing feature maps from various levels of the pyramid, the head performs detection through bounding box predictions, class probabilities, and object scores. In the final stage, the output layer processes a set of anchor boxes with various aspect ratios and scales. Each anchor is then combined with position and size offset predictions calculated relative to the grid cell, resulting in the final bounding box. In addition, the model also predicts an objectness score for each anchor, which represents the likelihood of an object's presence. This score serves to filter out irrelevant predictions, thereby improving detection precision. (Xie et al., 2024).

Predefined anchor boxes in detection models are often sensitive to object scale variations. Small anchors tend to have difficulty recognizing large objects, while large anchors are less accurate in detecting small objects. In addition, mismatches in aspect ratio between anchors and object shapes can reduce detection performance. Therefore, selecting anchor boxes that match object characteristics is an important factor in improving detection accuracy (Zheng et al., 2023). One simpler and more efficient approach to determining the initial anchor is the K-Means algorithm, which clusters data based on the distance to the cluster center (prototype), thereby representing the size and shape of the dominant objects in the dataset (Tang et al., 2024).

In the YOLOv7-Tiny architecture, the initial anchor box scale is designed based on the COCO dataset (Hu et al., 2023). However, when applied to the UAV dataset, this scale is unable to represent the entire range of object sizes, which slows down the parameter training process and reduces detection speed. To overcome this limitation, a modification of YOLOv7-Tiny was developed with the application of a Manhattan distance-based K-Means algorithm (Shim et al., 2022). Manhattan distance is a calculation method that measures the absolute difference between the coordinates of two objects (Asgar et al., 2023). This algorithm is used to determine a more appropriate initial anchor box scale that is capable of covering the entire object scale in the UAV dataset (Xue et al., 2022).

Therefore, in this study, YOLOv7-tiny is used as a baseline to be developed to improve the detection of small objects in UAV images through architectural modifications and contributions:

- Proposing modifications to the YOLOv7-Tiny architecture by adding high-resolution detection paths and scales to improve detection performance.
- Adjusting anchor box configuration using the Manhattan distance-based K-means method based on object size distribution in UAV images.
- Conducting a comprehensive evaluation of the influence of architectural modifications and anchors on detection performance.

2 METHODOLOGY

2.1 Dataset

This study utilizes a combined dataset from three main sources for vehicle detection in UAV images (Muzammul et al., 2024). The first source is the aerial-cars dataset, which consists of 153 annotated images (Butler & Leung, 2024). The second source, the M0606 subset of the UAV Detection and Tracking Benchmark (UAVDT) (Du et al., 2023), includes 1,255 images with a variety of viewing angles, lighting, and backgrounds. The third source consists of 157 images extracted and manually annotated from videos with a resolution of 2720×1530 pixels at 30 fps, recorded using a DJI Phantom 4 Pro drone (P. Wang et al., 2024).

All images are annotated in YOLO format, with five parameters relative to image size: class ID, center coordinates (x, y), width, and height of the bounding box. The dataset includes four object classes, namely car, truck, bus, and minibus, and is randomly divided into 90% training data and 10% test data.

2.2 YOLOv7-Tiny Architecture

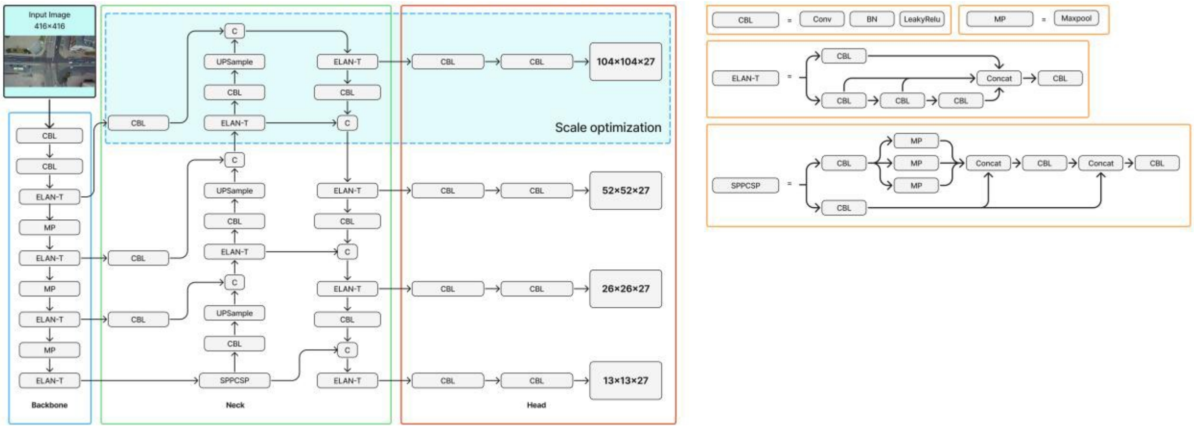

Figure 1: YOLOv7-Tiny Architecture with Scale Optimization.

In this study, a small object detection model was developed using YOLOv7-Tiny as its basis. YOLOv7-Tiny has a concise model structure and high inference speed, making it suitable for use on devices with limited resources (Cheng et al., 2024). However, the model's detection of small objects in images with complex backgrounds still needs to be improved and requires further optimization and refinement (Gong et al., 2022).

Because YOLOv7-Tiny has a lightweight architecture and is suitable for running on edge GPUs (R. Liu et al., 2024), this study uses 416×416 pixel RGB image inputs. This size was chosen to reduce the computational load and speed up the inference process, making it more efficient than the standard 640×640 pixel size (LU et al., 2023) and consists of three main components, namely the backbone, neck, and head (D. Cao et al., 2025). The backbone acts as a feature extraction layer and consists of several main modules, namely Convolution-BatchNorm-LeakyReLU (CBL) (Gong et al., 2024), Efficient Layer Aggregation Network (ELAN-T) (Lee et al., 2024), and Max-Pooling (MP) (Deepti Raj & Prabadevi, 2024). The CBL module, which consists of convolution layers, batch normalization, and the Leaky ReLU activation function, serves to extract feature information from images. Meanwhile, the ELAN module is built by combining several CBL blocks through branching paths, thereby increasing the network's learning capacity. The MP module uses max-pooling operations to perform downsampling and reduce feature dimensions (Chen et al., 2024).

The neck serves as a feature concatenator by utilizing the SPPCSP (X. Cao et al., 2024), CBL, and ELAN-T modules. The SPPCSP module consists of Spatial Pyramid Pooling (SPP) (Dewi et al., 2023), which uses max-pooling at multiple scales to capture cross-resolution information, and Cross Stage Partial (CSP) (Dewi & Juli Christanto, 2022), which performs concatenation to enrich feature representations. This neck structure adopts the Path Aggregation Feature Pyramid Network (PAFPN) (Ang et al., 2024) approach, which flows feature information top-down and bottom-up to strengthen multi-scale detection. In this study, optimization was performed on the neck by adding a new extraction path from one of the ELAN-T layers in the backbone to the head, forming an additional 104×104 pixel detection layer. The addition of this path allows for more optimal utilization of high-resolution feature flow, giving the model better sensitivity to small objects that are often missed in standard configurations.

With optimization as shown in Figure 1, the head layer now has four detection scales, namely 104×104, 52×52, 26×26, and 13×13. With the addition of new detection scales, the configuration in the head section must also be adjusted, particularly in relation to the number of output channels generated at each scale. This is important because each feature map in the head is tasked with generating predictions in the form of bounding boxes, confidence, and object classes. Therefore, the number of output channels at each scale is determined using the equation:

Output channel = number of anchors x (5 + C) (1)

Where 5 represents the bounding box coordinates (x, y, w, h) and confidence, while C is the number of classes. For example, in the COCO dataset which has 80 classes, the calculation becomes 3×(5+80)=255, resulting in outputs of 52×52×255, 26×26×255, and

13×13×255. Meanwhile, this study uses four classes, so the number of output channels is 3×(5+4)=27. Thus, the four optimized detection scales, namely 104×104×27, 52×52×27, 26×26×27, and 13×13×27, have produced outputs that correspond to the number of classes in this study's dataset, as shown in Figure 2.

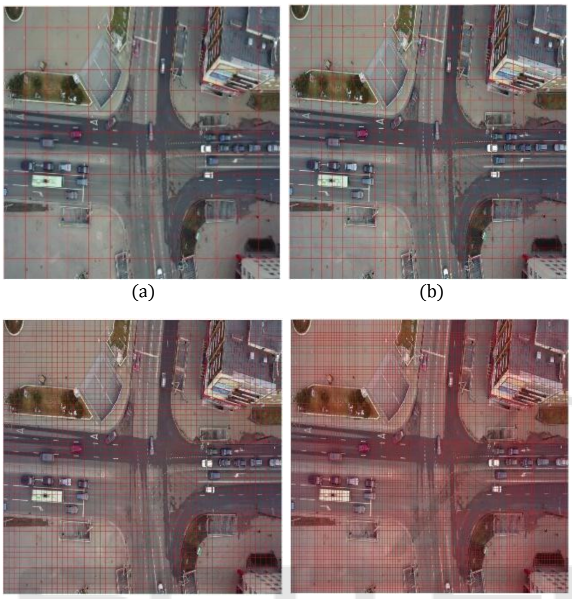
(a) (b)

(c) (d)

Figure 2: Illustration of multi-scale grid cells in the optimized YOLOv7-Tiny for UAV object detection: (a) 13x13x27, (b) 26x26x27, (c) 52x52x27, (d) 104x104x27.

2.3 Anchor Boxes YOLOv7-Tiny

Anchor boxes are predefined bounding boxes used by YOLO as references in predicting the presence of objects. Each YOLO detection path uses three anchor boxes (nine boxes in total), with outputs measuring 52×52×255, 26×26×255, and 13×13×255 (Limberg et al., 2022). These three scales of feature maps are used to detect objects of different sizes, where 52×52 is for small objects, 26×26 is for medium-sized objects, and 13×13 is for large objects. In the optimized YOLOv7-Tiny architecture, an additional detection path at a scale of 104×104 is introduced to improve performance in detecting very small objects.

As a result, the model now uses four scales of feature maps (104×104, 52×52, 26×26, and 13×13). Since each scale uses three pairs of anchor boxes (width and height), the total number of anchor boxes used is 12 centroids. To determine the initial values of these 12 centroids, the k-means clustering algorithm is used. In the initial stage, each bounding box in the dataset is assigned to the nearest centroid by calculating the distance between the width and height of the bounding box and the centroid using the Manhattan distance formula (2) as follows:

$$D(x,y) = | x_i - y_i | + | x_j - y_j | \quad (2)$$

Where (x_i , x^j) represents the width and height of the bounding box, and (y_i, y_j) represents the centroid coordinates. After this initial classification, each centroid is updated by calculating the average dimensions of all bounding boxes in its cluster, expressed as:

$$C_k = \frac{1}{n}\sum_{i=1}^{n} x_1 \quad (3)$$

Where $C_k$is the new centroid for cluster k, $n$is the number of bounding boxes in the cluster, and x_i is the dimension of the i-th bounding box. This clustering and updating process is repeated iteratively until the centroids converge or no longer undergo significant changes. Once convergence has been achieved, as shown in Figure 3, the centroids are sorted by size from smallest to largest, as shown in Table 1. Then mapped to four scales of the feature map. Thus, each scale obtains three pairs of anchor boxes corresponding to the size range of the target objects. The resulting anchors are ready for use in the optimized YOLOv7-Tiny model, thereby improving detection performance, especially for small objects.

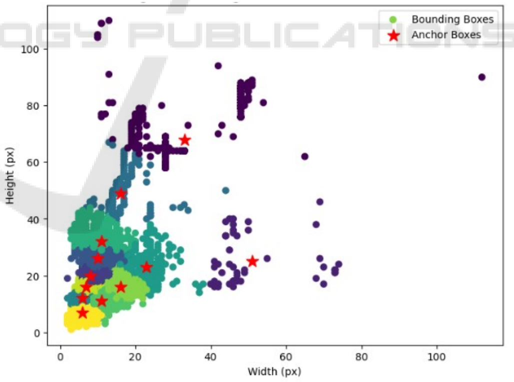

Figure 3: Anchor Distribution from Manhattan Distance Clustering.

2.4 Evaluation

The evaluation was conducted on a test dataset consisting of 10% of the total combined dataset, including the aerial-cars dataset (153 annotated images), the M0606 subset of the UAV Detection and Tracking Benchmark (UAVDT) containing 1,255 images with variations in viewpoint, lighting, and background, and 157 images extracted from private

Table 1: Anchor box dimensions obtained from clustering.

Anchor Index	Width (px)	Height (px)	Area (px^2)
1	6	7	42
2	6	12	72
3	7	16	112
4	11	11	121
5	9	20	180
6	16	16	256
7	10	26	260
8	11	32	352
9	23	23	529
10	16	49	784
11	51	25	1.275
12	33	68	2.244

UAV recordings with a resolution of 2720×1530 pixels at 30 fps. This dataset was selected randomly so that it still represents the variation in object size and image capture conditions commonly found in UAV images. Model performance is evaluated using the metrics Precision (P), Recall (R), and F1 Score (F1) (Sathyanarayanan & Tantri, 2024) with the following formula:

$$P = \frac{TP}{TP+FP} \tag{4}$$

$$R = \frac{TP}{TP+FN} \tag{5}$$

$$F1 = \frac{2PR}{P+R} \tag{6}$$

3 RESULTS

3.1 Experimental Setup

The entire training process was conducted on the Google Colab platform with NVIDIA Tesla T4 GPU support (16 GB VRAM), which enabled efficient training of the YOLOv7-Tiny model. This training environment was chosen because it provides sufficient computing resources for deep learning-based object detection experiments without requiring additional local infrastructure.

3.2 Object Detection Performance

Table 2: Comparison of detection performance and inference time between Baseline YOLOv7-Tiny and Optimized YOLOv7-Tiny.

Metrics	Baseline YOLOv7-Tiny		Optimized YOLOv7-Tiny	
	Performance	Detection Time	Performance	Detection Time
Precision	95	-	95	-
Recall	96	-	96	-
F1-Score	95	-	96	-
mAP@50	96.73	4 seconds	97.46	6 seconds
mAP@55	96.11	5 seconds	96.72	7 seconds
mAP@60	95.34	6 seconds	95.82	5 seconds
mAP@65	93.06	5 seconds	94.62	6 seconds
mAP@70	90.18	5 seconds	92.26	6 seconds
mAP@75	86.28	4 seconds	85.73	6 seconds
mAP@80	76.24	4 seconds	77.73	5 seconds
mAP@85	55.84	4 seconds	60.49	6 seconds
mAP@90	24.74	4 seconds	25.32	7 seconds
mAP@95	2.34	4 seconds	1.22	6 seconds
mAP@50- 95	71.68	4 seconds	72.73	6 seconds

The results of the evaluation matrix comparison in Table 2 show that both models achieved the same precision and recall values of 95 and 96, respectively. However, Optimized YOLOv7-Tiny showed an increase in F1-Score from 95 to 96, which represents better detection performance consistency as a result of optimizing the relationship between precision and recall. In the mean Average Precision metric, the optimized model provides improvements at low to medium IoU thresholds, with mAP@50 increasing from 96.73 to 97.46, mAP@70 rising from 90.18 to 92.26, and mAP@85 from 55.84 to 60.49. However, performance decreased at high IoU thresholds, with mAP@95 dropping from 2.34 to 1.22. But overall, the average mAP@50–95 value increased from 71.68 to 72.73, indicating an improvement in detection performance.

In terms of inference time, the baseline model is faster with an average of four to six seconds, while the optimized model takes five to seven seconds. This shows a trade-off between improved detection accuracy and processing time efficiency.

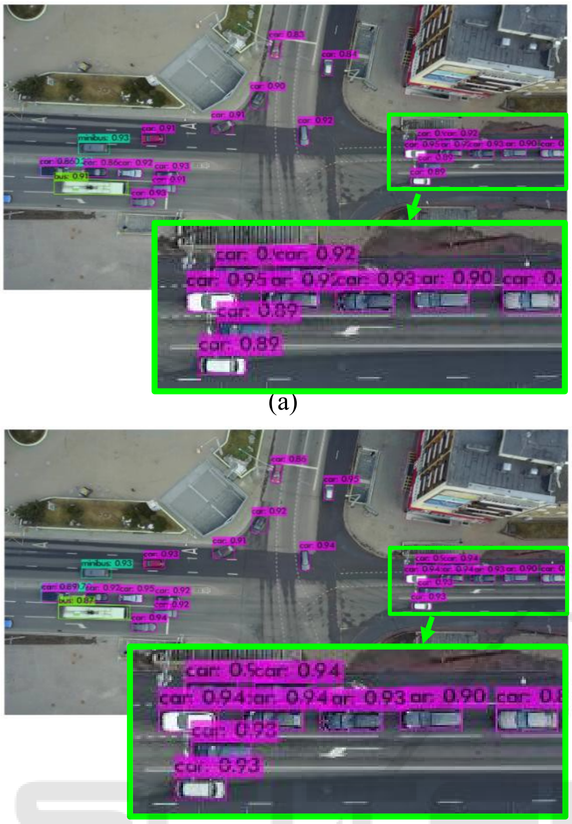

Figure 4: Detection Results on UAV Images: (a) Baseline YOLOv7-Tiny and (b) Optimized YOLOv7-Tiny.

The detection results in Figure 4 show differences in detection quality between the two models. The baseline YOLOv7-Tiny still tends to miss some small objects and produces relatively lower confidence scores. In contrast, Optimized YOLOv7-Tiny is able to detect the same objects with a more consistent and higher confidence level. This phenomenon is clearly visible in areas with high vehicle density, where the optimized model provides more stable detection. Thus, these visual results are consistent with the quantitative findings in the evaluation metrics, which overall show an improvement in detection performance.

4 DISCUSSION

The evaluation results show that the optimization carried out in this study produced varying performance changes. In the evaluation metrics, precision and recall did not change, but there was a slight increase in the F1-Score value. This increase indicates a better balance between precision and recall, resulting in more consistent detection performance. A more significant difference was seen in the mean Average Precision metric. The optimized model showed improved performance at low to medium IoU thresholds, while performance decreased at high IoU thresholds. This phenomenon indicates that the model is quite good at detecting objects at low thresholds, and is even more optimal in the optimized model. However, both models still experience a decline in performance at high thresholds, with relatively low mAP values, namely 2.34 for the baseline model and 1.22 for the optimized model. This indicates that the model still faces difficulties in producing truly accurate bounding box predictions, even though the objects have been successfully detected.

The improvement in mAP is inseparable from the anchor optimization performed using the k-means algorithm with Manhattan distance. This strategy produces anchors that are more representative of the distribution of object sizes in the dataset, enabling the model to produce more accurate bounding box predictions. In addition, modifications to the YOLOv7-Tiny architecture carried out in this study, namely through the addition of a feature fusion/aggregation layer in the neck and the addition of an extra detection layer in the head to accommodate small objects, also influenced the detection results. However, these architectural changes had an impact on increasing the inference time, where the optimized model took longer than the baseline model. Thus, it can be concluded that there is a trade-off between improved detection accuracy and processing time efficiency.

5 CONCLUSION

This study shows that optimizing the YOLOv7-Tiny architecture and anchors using k-means and Manhattan Distance can improve the detection of small objects in UAV images. The evaluation results show a better F1-Score and an increase in mAP at low to medium IoU thresholds, with an average mAP@50–95 increasing from 71.68 to 72.73. However, performance at high IoU thresholds still declined and inference time became longer due to the addition of feature fusion paths and new detection scales. Overall, this study succeeded in improving small object detection, although there are still limitations in high precision that could be the focus of further research.

REFERENCES

Ali, M. L., & Zhang, Z. (2024). The YOLO Framework: A Comprehensive Review of Evolution, Applications, and Benchmarks in Object Detection. In *Computers* (Vol. 13, Issue 12). Multidisciplinary Digital Publishing Institute (MDPI). https://doi.org/10.3390/computers13120336

Ang, L., Rahim, S. K. N. A., Hamzah, R., Aminuddin, R., & Yousheng, G. (2024). *YOLO algorithm with hybrid attention feature pyramid network for solder joint defect detection*. http://arxiv.org/abs/2401.01214

Asgar, M. R. G., Hidayat, R., & Bejo, A. (2023). Comparison Euclidean Distance and Manhattan Distance as Classification in Speech Recognition System. In *Proceedings of the International Conference on Educational Management and Technology (ICEMT 2022)* (pp. 454–463). Atlantis Press SARL. https://doi.org/10.2991/978-2- 494069-95-4_54

Badgujar, C. M., Poulose, A., & Gan, H. (2024). *Agricultural Object Detection with You Look Only Once (YOLO) Algorithm: A Bibliometric and Systematic Literature Review.*

Bi, H., Wen, V., & Xu, Z. (2023). Comparing one- stage and two-stage learning strategy in object detection. *Applied and Computational Engineering*, *5*(1), 171–177. https://doi.org/10.54254/2755-2721/5/20230556 Butler, J., & Leung, H. (2024). A Heatmap-Supplemented R-CNN Trained Using an Inflated IoU for Small Object Detection. *Remote Sensing*, *16*(21). https://doi.org/10.3390/rs16214065

Cao, D., Luo, W., Tang, R., Liu, Y., Zhao, J., Li, X., & Yuan, L. (2025). Research on Apple Detection and Tracking Count in Complex Scenes Based on the Improved YOLOv7-Tiny-PDE. *Agriculture (Switzerland)*, *15*(5). https://doi.org/10.3390/agriculture15050483

Cao, X., Xu, Y., He, J., Liu, J., & Wang, Y. (2024). A Lightweight Traffic Sign Detection Method With Improved YOLOv7-Tiny. *IEEE Access*, *12*, 105131–105147. https://doi.org/10.1109/ACCESS.2024.3435384

Chen, Z., Qian, M., Zhang, X., & Zhu, J. (2024). Chinese Bayberry Detection in an Orchard Environment Based on an Improved YOLOv7-Tiny Model. *Agriculture (Switzerland)*, *14*(10). https://doi.org/10.3390/agriculture14101725

Cheng, D., Zhao, Z., & Feng, J. (2024). Rice Diseases Identification Method Based on Improved YOLOv7-Tiny. *Agriculture (Switzerland)*, *14*(5). https://doi.org/10.3390/agriculture14050709

Deepti Raj, G., & Prabadevi, B. (2024). MoL-YOLOv7: Streamlining Industrial Defect Detection With an Optimized YOLOv7 Approach. *IEEE Access*, *12*, 117090–117101. https://doi.org/10.1109/ACCESS.2024.3447035

Dewi, C., Chen, R.-C., Yu, H., & Jiang, X. (2023). *Robust Detection Method for Improving Small Traffic Sign Recognition Based on Spatial Pyramid Pooling.*

Dewi, C., & Juli Christanto, H. (2022). Combination of Deep Cross-Stage Partial Network and Spatial Pyramid Pooling for Automatic Hand Detection. *Big Data and Cognitive Computing*, *6*(3). https://doi.org/10.3390/bdcc6030085

Du, B., Huang, Y., Chen, J., & Huang, D. (2023). *Adaptive Sparse Convolutional Networks with Global Context Enhancement for Faster Object Detection on Drone Images*. https://github.com/Cuogeihong/CEASC.

Gong, H., Ma, X., & Guo, Y. (2024). Research on a Target Detection Algorithm for Common Pests Based on an Improved YOLOv7-Tiny Model. *Agronomy*, *14*(12). https://doi.org/10.3390/agronomy14123068

Gong, H., Mu, T., Li, Q., Dai, H., Li, C., He, Z., Wang, W., Han, F., Tuniyazi, A., Li, H., Lang, X., Li, Z., & Wang, B. (2022). Swin-Transformer-Enabled YOLOv5 with Attention Mechanism for Small Object Detection on Satellite Images. *Remote Sensing*, *14*(12). https://doi.org/10.3390/rs14122861

Hu, S., Zhao, F., Lu, H., Deng, Y., Du, J., & Shen, X. (2023). Improving YOLOv7-Tiny for Infrared and Visible Light Image Object Detection on Drones. *Remote Sensing*, *15*(13). https://doi.org/10.3390/rs15133214

Lee, J. H., Choi, Y. H., Lee, H. S., Park, H. J., Hong, J. S., Lee, J. H., Sa, S. J., Kim, Y. M., Kim, J. E., Jeong, Y. D., & Cho, H. C. (2024). Enhanced Swine Behavior Detection with YOLOs and a Mixed Efficient Layer Aggregation Network in Real Time. *Animals*, *14*(23). https://doi.org/10.3390/ani14233375

Limberg, C., Melnik, A., Harter, A., & Ritter, H. (2022). *YOLO -- You only look 10647 times*. http://arxiv.org/abs/2201.06159

Liu, R., Huang, M., Wang, L., Bi, C., & Tao, Y. (2024). PDT-YOLO: A Roadside Object- Detection Algorithm for Multiscale and Occluded Targets. *Sensors*, *24*(7). https://doi.org/10.3390/s24072302

Liu, S., Shao, F., Chu, W., Zhang, H., Zhao, D., Xue, J., & Liu, Q. (2025). LCM-YOLO: A Small Object Detection Method for UAV Imagery Based on YOLOv5. *IET Image Processing*, *19*(1). https://doi.org/10.1049/ipr2.70051

Lu, Guozhen, Xiong, X., & Lu, D. (2023). *Research on Visualization Method of Edge Banding Appear- ance Quality Based on YOLOv7*. https://doi.org/10.21203/rs.3.rs-3279477/v1

Mohsan, S. A. H., Khan, M. A., Noor, F., Ullah, I., & Alsharif, M. H. (2022). Towards the Unmanned Aerial Vehicles (UAVs): A Comprehensive Review. In *Drones* (Vol. 6, Issue 6). Multidisciplinary Digital Publishing Institute (MDPI). https://doi.org/10.3390/drones6060147

Muzammul, M., Algarni, A., Ghadi, Y. Y., & Assam, M. (2024). Enhancing UAV Aerial Image Analysis: Integrating Advanced SAHI Techniques with Real-Time Detection Models on the VisDrone Dataset. *IEEE Access*, *12*, 21621–21633. https://doi.org/10.1109/ACCESS.2024.3363413

Sathyanarayanan, S., & Tantri, B. R. (2024). Confusion Matrix-Based Performance Evaluation Metrics. *African Journal of Biomedical Research*, 4023–4031. https://doi.org/10.53555/ajbr.v27i4s.4345

Shim, Y., Choi, S. W., Yang, M. G., Chung, K. Y., & Baek, K. H. (2022). Energy Efficient Distance Computing: Application to K-Means Clustering. *Electronics (Switzerland)*, *11*(3). https://doi.org/10.3390/electronics11030298

Tang, H., Gao, S., Li, S., Wang, P., Liu, J., Wang, S., & Qian, J. (2024). A Lightweight SAR Image Ship Detection Method Based on Improved Convolution and YOLOv7. *Remote Sensing*, *16*(3). https://doi.org/10.3390/rs16030486

Telçeken, M., Akgun, D., & Kacar, S. (2024). An Evaluation of Image Slicing and YOLO Architectures for Object Detection in UAV Images. *Applied Sciences (Switzerland)*, *14*(23). https://doi.org/10.3390/app142311293

Wang, C.-Y., Bochkovskiy, A., & Liao, H.-Y. M. (2023). *YOLOv7: Trainable bag-of-freebies sets new state-of-the-art for real-time object detectors*. https://github.com/

Wang, P., Wang, Y., & Li, D. (2024). *DroneMOT: Drone-based Multi-Object Tracking Considering Detection Difficulties and Simultaneous Moving of Drones and Objects*. http://arxiv.org/abs/2407.09051

Wang, Q., Zhang, Z., Chen, Q., Zhang, J., & Kang, S. (2024). Lightweight Transmission Line Fault Detection Method Based on Leaner YOLOv7- Tiny. *Sensors*, *24*(2). https://doi.org/10.3390/s24020565

Xiao, Y., & Di, N. (2024). SOD-YOLO: A lightweight small object detection framework. *Scientific Reports*, *14*(1), 25624. https://doi.org/10.1038/s41598-024-77513-4

Xie, M., Yang, X., Li, B., & Fan, Y. (2024). A YOLO-Based Method for Head Detection in Complex Scenes. *Sensors*, *24*(22). https://doi.org/10.3390/s24227367

Xu, X., Zhao, M., Shi, P., Ren, R., He, X., Wei, X., & Yang, H. (2022). Crack Detection and Comparison Study Based on Faster R-CNN and Mask R-CNN. *Sensors*, *22*(3). https://doi.org/10.3390/s22031215 Xue, J., Cheng, F., Li, Y., Song, Y., & Mao, T. (2022). Detection of Farmland Obstacles Based on an Improved YOLOv5s Algorithm by Using CIoU and Anchor Box Scale Clustering. *Sensors*, *22*(5). https://doi.org/10.3390/s22051790

Zhang, Z., Xie, X., Guo, Q., & Xu, J. (2024). Improved YOLOv7-Tiny for Object Detection Based on UAV Aerial Images. *Electronics (Switzerland)*, *13*(15). https://doi.org/10.3390/electronics13152969

Zheng, J., Zhao, S., Xu, Z., Zhang, L., & Liu, J. (2023). Anchor boxes adaptive optimization algorithm for maritime object detection in video surveillance. *Frontiers in Marine Science*, *10*. https://doi.org/10.3389/fmars.2023.1290931